MOLECULAR AND CELLULAR BIOLOGY, Feb. 1991, p. 803–812
0270-7306/91/020803-10$02.00/0

Vol. 11, No. 2

αB Crystallin Accumulation Is a Specific Response to Ha-*ras* and v-*mos* Oncogene Expression in Mouse NIH 3T3 Fibroblasts

ROMAN KLEMENZ,[1]* ERIKA FRÖHLI,[1] AKIRA AOYAMA,[1] SYLVIA HOFFMANN,[1]† RICHARD J. SIMPSON,[2] ROBERT L. MORITZ,[2] AND REINHOLD SCHÄFER[1]

Division of Cancer Research, Institute of Pathology, University Hospital, Schmelzbergstr. 12, CH-8091 Zurich, Switzerland,[1] and Joint Protein Structure Laboratory, Ludwig Institute for Cancer Research, and The Walter and Eliza Hall Institute for Medical Research, P.O. Royal Melbourne Hospital, Parkville, Victoria 3050, Australia[2]

Received 13 August 1990/Accepted 5 November 1990

The conditional expression of the v-*mos* and Ha-*ras*(EJ) oncogenes in NIH 3T3 cells leads to the accumulation of a 23-kDa protein (p23) (R. Klemenz, S. Hoffmann, R. Jaggi, and A.-K. Werenskiold, Oncogene 4:799–803, 1989). We purified p23 to homogeneity and determined part of the amino acid sequence. The obtained sequence is identical with that of the eye lens protein αB crystallin. Northern (RNA) blot and Western immunoblot experiments were performed to demonstrate that αB crystallin mRNA and protein do indeed accumulate as a consequence of v-*mos* and Ha-*ras* oncogene expression. Comparison of cDNA clones obtained from the mRNA of eye lenses and of oncogene-expressing fibroblasts revealed identity between them. The major transcription initiation site of the αB crystallin gene in our experimental system was shown by primer extension experiments to be identical with the one used in eye epithelial cells. In addition, we identified a second minor initiation site 49 nucleotides further upstream. Serum growth factors did not stimulate αB crystallin expression in growth-arrested cells.

Preneoplastic mouse NIH 3T3 fibroblasts can be converted to the malignant state by introduction of a single activated oncogene. Oncoprotein accumulation in NIH 3T3 cells results in morphological alterations, deregulation of growth, and tumorigenicity. NIH 3T3 cells have been extensively used as a model system to elucidate the complex cascade of biochemical events and alterations of gene expression associated with growth stimulation and neoplastic transformation. Phenotypically normal NIH 3T3 cells require stimulation by exogenous growth factors to enter and transverse the cell cycle. Growth of transformed NIH 3T3 cells is independent of external mitogenic stimuli.

Since oncoproteins and growth factors share the ability to trigger cell division, we expect them to induce a common panel of genes whose products are involved in proliferative processes. A large number of growth factor-regulated genes have been identified in the last few years (for recent reviews, see references 15 and 44). Many of them are indeed also regulated by oncoproteins. Among them are genes which encode growth factors (e.g., tumor growth factor α [7] and 9E3 [55]), proteases (e.g., transin [28], cathepsin L [14], and collagenase [48]), transcription factors (e.g., c-*fos* [54] and c-*jun* [52]), viral genes (e.g., VL 30 [39] and the polyomavirus enhancer [59]), and genes of unknown functions (e.g., T1 [22, 60] and pS2 [34]). However, in contrast to growth factors, oncoproteins not only trigger cell division but also induce additional changes such as altered cell morphology, anchorage-independent proliferation, and tumorigenicity. Microinjection of the oncogenic Ha-*ras* gene product into established cell lines revealed that the early events of transformation only occur under conditions of ongoing transcription and translation (13). This strongly suggests that the oncoprotein-mediated changes are not only mediated by deregulation of oncoprotein activity but are also catalyzed by proteins whose synthesis is induced through the action of oncoproteins. Some alterations might also be accounted for by the oncoprotein-mediated disappearance of some proteins. To unravel the pathways in which oncoproteins act, one can either search for the downstream targets upon which they impinge or study the signals which ultimately reach the nucleus by analyzing the molecular mechanisms which underlie the oncoprotein-mediated gene expression. We chose the second approach and set out to isolate a gene whose product is selectively synthesized in response to the expression of oncogenes. In two-dimensional gels, we have observed such proteins after the induced expression of the Ha-*ras* and v-*mos* oncogenes in NIH 3T3 mouse fibroblasts but not after serum stimulation of growth-arrested cells (21). To study the regulation of the induced synthesis of these proteins, we are in need of the cognate gene. Here we describe the isolation and identification of a 23-kDa protein whose synthesis is specifically induced in Ha-*ras* and v-*mos* oncogene-transformed cells but not by serum growth factors in serum-starved cells. This protein was identified as αB crystallin. We demonstrate that p23, expressed in NIH 3T3 fibroblasts, and αB crystallin, isolated from eye lenses, are identical.

MATERIALS AND METHODS

Cell lines and growth conditions. This study was performed with preneoplastic NIH 3T3 cells and with NIH 3T3 clones that were stably transfected with the v-*mos* or Ha-*ras*(EJ) oncogene under the transcriptional control of the mouse mammary tumor virus (MMTV) long terminal repeat (LTR) promoter (NIH[LTR-*mos*], NIH[LTR-*ras*(EJ)] [19]). Cells were grown in Dulbecco modified Eagle medium containing 10% fetal calf serum (FCS). Transcription of the transfected oncogenes was induced by the addition of dexamethasone to a final concentration of 1 μM. All experiments were performed with cells in the exponential growth phase.

* Corresponding author.
† Present address: Institute of Plant Physiology, University of Berne, Altenbergrain 21, CH-3013 Bern, Switzerland.

Protein labeling and purification of p23. NIH[LTR-*mos*] cells grown on 15-cm culture dishes were treated with 1 μM dexamethasone for 36 h. Cells were washed twice with phosphate-buffered saline (PBS) and swollen in 10 ml of 10 mM Tris hydrochloride (pH 8.0)–0.1 mM dithiothreitol (DTT)–1 mM phenylmethylsulfonyl fluoride on ice for 5 min. Cells were lysed in a Dounce homogenizer, and nuclei and cell debris were removed by centrifugation at 500 × *g* for 10 min. Particulate material was pelleted by centrifugation at 100,000 × *g* for 30 min and discarded. Soluble proteins were precipitated stepwise from the 100,000 × *g* supernatant (S100 fraction) by the addition of ammonium sulfate to 30 and 50% saturation. The proteins which precipitated between 30 and 50% saturated ammonium sulfate were further fractionated by electrophoresis through sodium dodecyl sulfate (SDS)-12.5% polyacrylamide gels (24). A strip of the gels was stained to localize the position of p23, and the corresponding region was cut out of the gels. Proteins were electroeluted and collected on dialysis membranes. Final purification was achieved by two-dimensional nonequilibrium gel electrophoresis (36) with an Ampholine mixture of pK 3.5 to 10 in the first dimension and SDS-12.5% polyacrylamide gels in the second dimension. The proteins were visualized by staining with Coomassie brilliant blue. The spots representing p23 were cut out of the gels, and the protein was electroeluted. For analytical purposes, NIH[LTR-*mos*] cells were grown on 10-cm culture dishes and either stimulated with dexamethasone for 8 h or left untreated. The medium was removed and replaced with 3 ml of methionine-free Dulbecco modified Eagle medium to which 0.9 mCi of [^{35}S]methionine (800 Ci/mmol; Amersham) was added. After a labeling period of 90 min, the medium was removed and the cells were washed twice with PBS. Cell lysis and fractionation were performed as described above. The ammonium sulfate precipitates were dissolved in sample buffer for two-dimensional gels (9.5 M urea, 2% Nonidet P-40, 2% Ampholines pH 3.5 to 10, 5% 2-mercaptoethanol) (35). Incorporation of radioactive methionine into proteins was determined by trichloroacetic acid precipitation. Proteins containing 10^6 cpm of incorporated methionine were subjected to analysis by two-dimensional nonequilibrium gel electrophoresis. The gels were impregnated with 2,5-diphenyloxazole (PPO) (4), and fluorograms were obtained by using Fuji RX films.

Silver staining of SDS-polyacrylamide gels was performed as described by Morrissey (30).

Western immunoblots. Protein extracts were prepared as described in the previous section. The ammonium sulfate precipitates were dissolved either in SDS sample buffer (80 mM Tris hydrochloride [pH 6.8], 100 mM DTT, 2% SDS, 10% glycerol, 0.2 mg of bromophenol blue per ml) or in sample buffer for two-dimensional gels. To determine the protein concentration, aliquots of the extracts in SDS sample buffer were spotted onto nitrocellulose and stained with amido black by the method of Schaffner and Weissmann (47). After destaining, the protein-bound dye was eluted and quantitated spectrophotometrically. Ten or 50 μg of protein was separated on 0.7- or 2-mm-thick SDS-12.5% polyacrylamide gels, respectively, and was electrophoretically transferred onto nitrocellulose membranes. The primary antiserum used to detect αB crystallin was raised against a decapeptide representing the carboxy terminus of lens αB crystallin (generously provided by J. Horwitz). The antiserum was used at a dilution of 1:300. As a secondary antibody, anti-rabbit immunoglobulin G coupled to alkaline phosphatase (Promega) was used. Immunocomplexes were visualized enzymatically by immersing the blots in 100 mM Tris hydrochloride (pH 9.5)–100 mM NaCl–5 mM $MgCl_2$–33 μg of Nitro Blue Tetrazolium per ml–16 μg of 5-bromo-4-chloro-3-indolyl phosphate per ml.

Amino acid sequence analysis. For sequence analysis, p23 was recovered from the electroeluate (approximately 500 μl) and freed of SDS and acrylamide gel contaminants by inverse-gradient reversed-phase high-performance liquid chromatography as described elsewhere (49). In brief, the p23 electroeluate (approximately 500 μl containing 5.3% SDS) was concentrated fivefold by centrifugal lyophilization (Savant Instruments, Inc., Hicksville, N.Y.), diluted to 1.3 ml with neat *n*-propanol in a sample-loading syringe, thoroughly mixed, and loaded onto an ODS-Hypersil column (5-μm particle size; 100 by 2.1 mm inner diameter) which had been previously equilibrated with 90% *n*-propanol–10% water. p23 was eluted with 50% *n*-propanol containing 0.4% trifluoroacetic acid. Chromatography was performed with a Perkin-Elmer model LC4 liquid chromatograph equipped with a variable-wavelength spectrometer (model LC95) and an LS4 fluorimeter. Samples were injected via a Rheodyne model 7125 septumless injection valve equipped with a 2-ml injection loop. Proteins were detected by their A_{280} and by fluorescence at 280-nm excitation and 340-nm emission.

Automated Edman degradation of p23 was performed with an Applied Biosystems sequencer (model 470A) equipped with an on-line phenylthiohydantoin amino acid analyzer (model 120A). Polybrene was used as a carrier.

In situ cyanogen bromide cleavage. After p23 (4 to 5 μg, approximately 160 pmol) had been subjected to four cycles of Edman degradation in the protein sequencer without any detectable phenylthiohydantoin-amino acids, the sequence analysis was stopped. In situ cyanogen bromide cleavage of native p23 was performed on the glass fiber disk of the protein sequencer by a procedure previously described (50, 51).

Preparation of mouse eye lens protein extracts. Isolated mouse eye lenses were either directly dissolved in SDS sample buffer and boiled for 5 min or lysed by swelling in hypotonic buffer (10 mM Tris hydrochloride [pH 8.0], 0.1 mM DTT, 1 mM phenylmethylsulfonyl fluoride). Insoluble material was removed by centrifugation.

Oligonucleotides. The following oligonucleotides were used: GGGCTGGAGAGAATAAGCTCAGAGCCGTGAG GC for Northern (RNA) blot hybridization and to determine the major transcription initiation site; GCAGCAGCTCCAG CCGGCCCCTTATATATGC to map the minor initiation site; and AACCGACTCTGCATTCATCTAGCCACAATG and CACTAGTCGACTCGAGT$_{15}$ as the sense-strand and antisense-strand primers, respectively, for the polymerase chain reaction (PCR). The oligonucleotides were purified on oligonucleotide purification cartridges (Applied Biosystems) or on Quiagen columns (Diagene) as described by the manufacturers. A 100-ng sample of oligonucleotide was radioactively labeled in 20 μl of 50 mM Tris hydrochloride (pH 7.6)–10 mM $MgCl_2$–5 mM DTT–0.1 mM EDTA–0.1 mM spermidine containing 80 μCi of [γ-^{32}P]ATP (5,000 Ci/mmol; Amersham) and with 9 U of T4 polynucleotide kinase (Boehringer) at 37°C for 1 h. Following the labeling reaction, the oligonucleotides used for primer extension experiments were purified on 8% polyacrylamide gels in TBE buffer (90 mM Tris borate, 90 mM boric acid, 2 mM EDTA) containing 8 M urea. The oligonucleotides used for hybridization to Northern blots were freed of radioactive ATP by passage through a Sephadex G-25 column.

Northern blots. RNA was purified by the acid guanidinium

thiocyanate-phenol-chloroform extraction method (5). Total RNAs (5 μg) were glyoxylated and fractionated on 1% agarose gels by the method of McMaster and Carmichael (29). Gels were stained with acridine orange, destained, and blotted onto nylon membranes (Biodyne; Pall Ultrafine Filtration Corporation). The filters were hybridized in 50% deionized formamide–10× Denhardt solution–50 mM Tris hydrochloride (pH 7.5)–1 M NaCl–10% dextran sulfate–200 μg of denatured herring sperm DNA–1 × 10^6 to 2 × 10^6 cpm of oligonucleotide or restriction fragment per ml at 42°C for 16 h. The final wash of the filters was in 0.2× SSC (1× SSC is 0.15 M NaCl plus 0.015 M sodium citrate)–0.1% SDS at 55°C. Restriction fragments containing specific v-*mos*, c-*fos*, human β-actin, and T1 gene sequences were labeled by the random oligonucleotide priming technique (11, 12).

Primer extension. The RNA used for primer extension experiments was extracted from NIH[LTR-*mos*] cells which were treated for 8 h with 1 μM dexamethasone before lysis. Oligonucleotide (40 fmol; 50,000 cpm) was mixed with 25 μg of total RNA in 25 μl of 50% formamide–400 mM NaCl–10 mM PIPES [piperazine-*N*,*N*′-bis(2-ethanesulfonic acid)] (pH 6.4)–1 mM EDTA and incubated at 80°C for 3 min. After annealing at 37°C for 16 h, the mixture was diluted 10-fold with cold water and nucleic acids were precipitated with isopropanol. The primer extension reaction was performed in 10 μl of 50 mM Tris hydrochloride (pH 8.0)–50 mM KCl–5 mM $MgCl_2$–5 mM DTT–0.1 mg of actinomycin D per ml–0.1 mM each deoxynucleoside triphosphate–7 U of avian myeloblastosis virus reverse transcriptase (Boehringer) at 42°C for 1 h. For the dideoxy-chain termination reaction (46), the conditions used were identical to the above-described primer extension reaction with the following changes: the concentration of each of the three driver deoxynucleoside triphosphates (not in competition with the dideoxynucleoside triphosphate) was 10 μM, the concentration of the deoxynucleoside triphosphate which was competed for by the corresponding dideoxynucleoside triphosphate was 6 μM, ddATP was 10 μM, ddCTP was 5 μM, ddGTP was 3 μM, and ddTTP was 1 μM. At the end of the reaction, NaOH was added to a final concentration of 0.1 N and the RNA was degraded by boiling for 5 min. After neutralization with HCl, DNA was ethanol precipitated and analyzed on 8% polyacrylamide sequencing gels (45).

Cloning and sequence analysis of αB crystallin cDNA. Total RNA was prepared from mouse brains, lungs, hearts, and eye lenses as well as from NIH[LTR-*mos*] cells which were treated with 1 μM dexamethasone for 24 h. cDNA was synthesized with 3 μg of RNA in 20 μl of 50 mM Tris hydrochloride (pH 8.3)–60 mM NaCl–6 mM magnesium acetate–10 mM DTT–50 pmol of an oligo(dT) adaptor primer consisting of 16 nucleotides with three hexanucleotide restriction enzyme recognition sites followed by a stretch of 15 dTs. The reaction was performed with 4 U of avian myeloblastosis virus reverse transcriptase at 42°C for 60 min. As the sense-strand primer for the PCR, we used a 30-mer oligonucleotide which can hybridize to nucleotides +19 to +48. The antisense-strand primer was the same as the cDNA synthesis adaptor primer. For the PCR, we used 5 μl of the cDNA synthesis mix in 50 μl of 10 mM Tris hydrochloride (pH 8.3)–50 mM KCl–5 mM $MgCl_2$–2% gelatin–200 μM deoxynucleoside triphosphates–5 pmol of both primers–5 U of Taq polymerase (Perkin-Elmer). The first reaction cycle consisted of 5 min at 95°C, 5 min at 50°C, and 30 min at 72°C and was followed by 35 cycles of 1 min at 94°C, 1 min at 55°C, and 2 min at 72°C. PCR-amplified cDNA was treated with T4 DNA polymerase cut with *Xho*I and cloned into the *Xho*I and *Sma*I sites of the cloning vector Bluescript SK+ (Stratagene). The two large *Bam*HI fragments of the cDNA (positions 71 to 413 and 429 to the *Bam*HI site in the polylinker of the vector) were subcloned in both orientations into the vector pBC SK+ (Stratagene). The nucleotide sequence of both strands of the cDNA was determined by the dideoxynucleoside triphosphate-chain termination reaction (46).

RESULTS

Purification and partial sequence determination of p23. We have previously described the induced synthesis of several proteins in NIH 3T3 cells upon the transcriptional activation of a transfected v-*mos* or Ha-*ras*(EJ) oncogene (21). These oncogenes were under the control of the MMTV promoter (MMTV-LTR) and hence could be induced with glucocorticoid hormones (19). To gain insight into the molecular mechanism underlying this oncoprotein-mediated induction, we needed to isolate the genes encoding those proteins. The isolation or identification of the corresponding genes required the purification of the proteins of interest. The protein with a molecular weight of 23,000, p23, was chosen for further studies because it belongs to the group of proteins whose accumulation was not induced by serum growth factors. Among the proteins of that group, it accumulated to the highest level. Particularly large amounts of p23 were synthesized in glucocorticoid-treated NIH 3T3 cells which contain a viral *mos* oncogene fused to the MMTV-LTR (NIH[LTR-*mos*]), whereas the response in Ha-*ras*-expressing cells was less pronounced (21).

A purification scheme was devised with radioactively labeled proteins. NIH[LTR-*mos*] cells were stimulated with dexamethasone for 8 h, or they were left untreated. Proteins were subsequently labeled with [^{35}S]methionine for 90 min before the lysis of the cells by hypotonic shock. The fractionation behavior of p23 was observed by two-dimensional gel electrophoresis. In the first step, a subcellular fraction free of nuclei and membranes was prepared by centrifugation at 100,000 × *g*. p23 in the high-speed supernatant (S100) was further enriched by precipitation at stepwise increased ammonium sulfate concentrations. Most of p23 precipitated between 30 and 50% ammonium sulfate saturation (Fig. 1A). For the large-scale preparation of p23, we followed the same purification scheme, followed by preparative SDS-polyacrylamide gel electrophoresis. Final purification was achieved on two-dimensional gels. Analysis of the p23 preparation by SDS-polyacrylamide gel electrophoresis revealed a single band upon silver staining (Fig. 1B).

Four cycles of Edman degradation of purified p23 (160 pmol) yielded no N-terminal sequence, indicating that the molecule was blocked at its amino-terminal end. The sequence analysis was halted, and p23 (immobilized on the sample disk of the sequencer) was then subjected to in situ cyanogen bromide treatment (50, 51). Sequence analysis was then continued and yielded a major amino acid sequence [Arg-Leu-Glu-X-Asp-Arg-Phe-Ser-Val-Asn-Leu-(Asp)-Val-] and a minor sequence [X-Ile-Ala-Ile-His-His-Pro-X-Ile-]. These data confirmed the notion that the N terminus of p23 was blocked and indicated the presence of at least two methionine residues in the molecule. Comparison of the obtained sequences with those of known proteins present in a data base revealed almost complete identity with sequences of the bovine, hamster, and human αB crystallin (Fig. 2). No sequence information for the mouse αB crystallin gene was available at that time. In the meantime, we

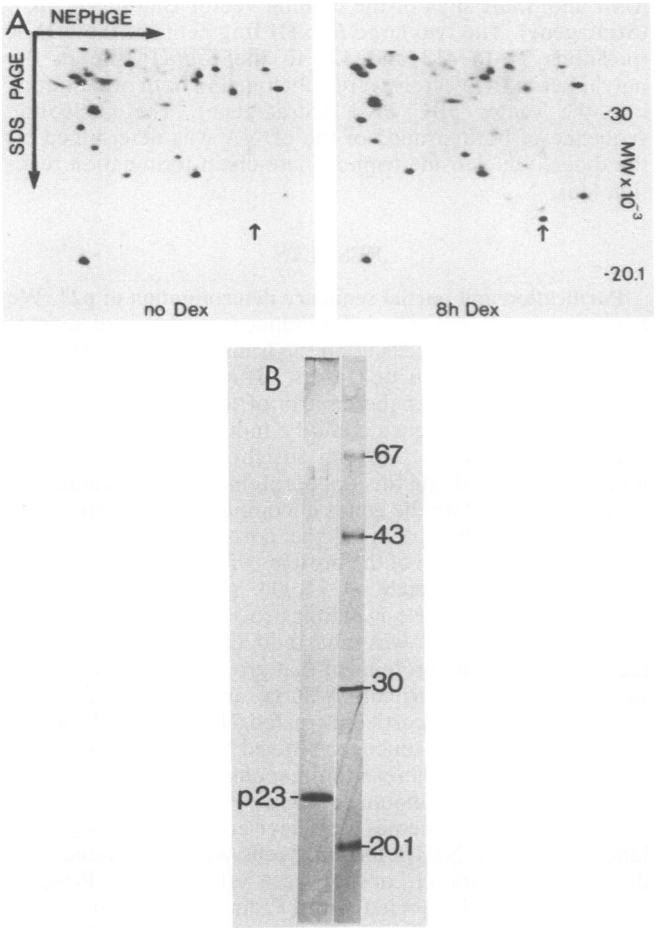

FIG. 1. Purification of p23. (A) NIH[LTR-*mos*] cells, untreated or stimulated for 8 h with dexamethasone (Dex), were labeled with [^{35}S]methionine for 90 min. The cells were lysed by hypotonic shock, an S100 supernatant was prepared, and the proteins were precipitated by stepwise addition of ammonium sulfate to 30, 50, and 80% saturation. The different precipitates were analyzed by two-dimensional nonequilibrium gel electrophoresis (NEPHGE). The proteins of the 30 to 50% ammonium sulfate cut were analyzed on the gels displayed in panel A. Only the relevant section of the gels is shown. The positions of the molecular weight (MW) markers are indicated. The arrows indicate the position of p23. (B) An aliquot of the purified p23 was analyzed on SDS-12.5% polyacrylamide gels and visualized by silver staining. The positions of the molecular weight markers ($\times 10^3$) are indicated at the side of the figure.

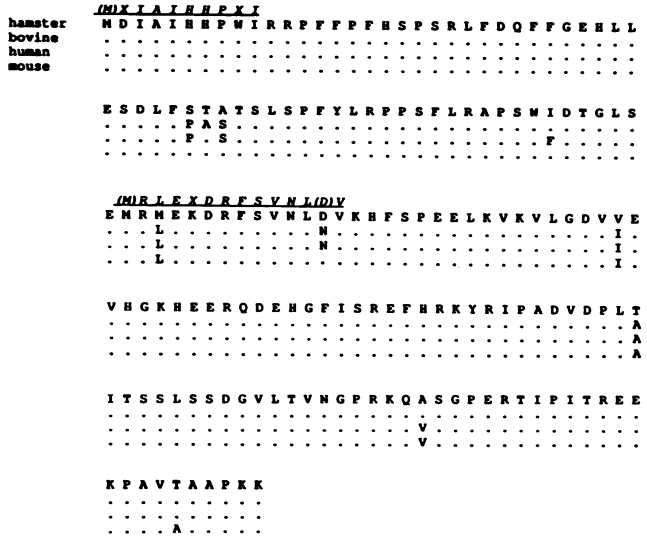

FIG. 2. Sequence alignment of the p23 BrCN cleavage products (underlined) and αB crystallin. Identities of the bovine (58), human (23), and mouse (this report, see Fig. 6) sequences with the hamster sequence (43) are indicated by dots. The X indicates unidentified amino acids. The parentheses around the aspartic acid in the second peptide signify uncertain amino acid assignment. The presence of the amino-terminal methionines of the two p23 peptides has been deduced from the ability of BrCN to cleave at these positions.

isolated and sequenced a mouse αB crystallin cDNA clone (Fig. 2; see Fig. 6). We observed complete identity between the deduced protein sequence and the identified sequences of p23.

These data, together with the fact that the molecular weight of p23 exactly corresponds to that of αB crystallin, strongly suggests identity between p23 and αB crystallin.

Detection of αB crystallin mRNA in v-*mos* oncogene-expressing cells. If p23 is indeed αB crystallin, we expect its cognate mRNA to accumulate in oncogene-expressing cells. The kinetics of v-*mos* mRNA accumulation in dexamethasone-stimulated NIH[LTR-*mos*] cells are shown in Fig. 3A. The hormone induced the transfected v-*mos* gene very rapidly and led to maximal mRNA levels within 3 h. The following rapid decline of v-*mos* mRNA was due to onco-protein-mediated feedback inhibition of the MMTV promoter (19). The transient expression of the v-*mos* gene resulted in the accumulation of αB crystallin mRNA (Fig. 3B). As an αB crystallin-specific hybridization probe, we used a radioactively labeled oligonucleotide which is complementary to a region of the mRNA near the transcription start site (9) (positions +16 to +49, see Fig. 5D, primer 1). Peak levels of αB crystallin mRNA were reached between 9 and 12 h. Only very small amounts of this mRNA were found at late times of dexamethasone stimulation in untransfected NIH 3T3 cells. A faint band migrating between the positions of 18S and 28S RNA was detected in some experiments. It is unlikely that this RNA encodes αB crystallin, as it was also present in uninduced cells and in dexamethasone-induced NIH cells, which do not synthesize detectable levels of this protein.

αB crystallin mRNA does not accumulate in response to growth stimulation of quiescent cells with serum. In a previous report, we have shown that the synthesis of p23 is not induced in serum-starved NIH 3T3 cells following growth stimulation with serum (21). To lend further support to the identity of p23 and αB crystallin, we searched for αB crystallin mRNA accumulation in response to serum stimulation. When NIH[LTR-*mos*] cells which were growth arrested for 24 h in a medium containing only 0.5% FCS were stimulated to reenter the cell cycle by the addition of 10% FCS, αB crystallin mRNA accumulation was not detected (Fig. 4). Effective growth stimulation was controlled for by rehybridizing the Northern blot with a probe which recognizes the mRNA of a serum-inducible gene. For this purpose, we chose the T1 gene, which is induced by serum, and the v-*mos* and Ha-*ras*(EJ) oncoproteins (22, 60) as well. The addition of 10% FCS clearly led to the transient synthesis of T1 mRNA (Fig. 4).

Transcription initiation sites of αB crystallin gene in v-*mos*-

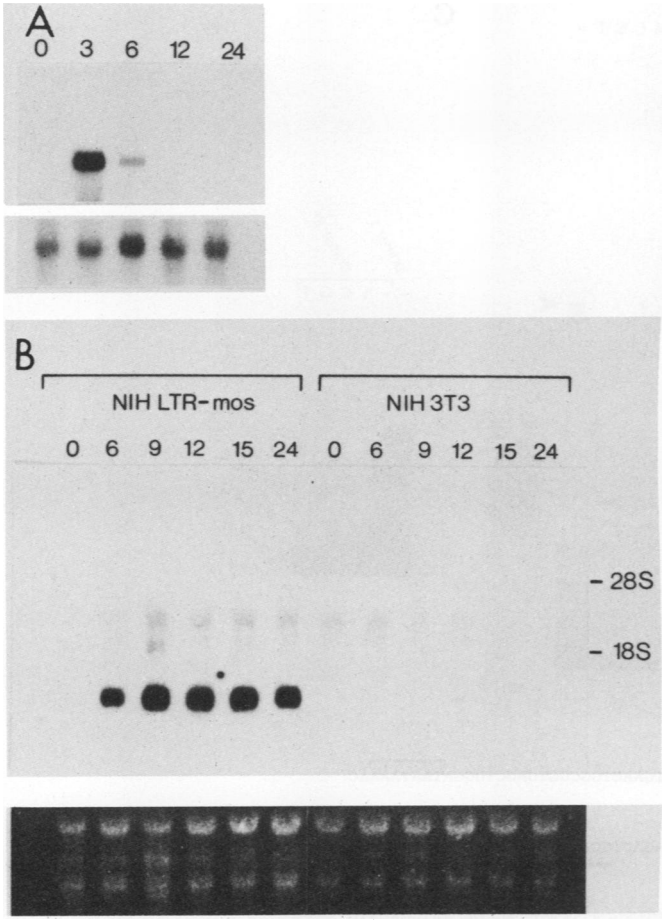

FIG. 3. Detection of αB crystallin mRNA in NIH[LTR-*mos*]-expressing cells. Total RNA was isolated from logarithmically growing NIH[LTR-*mos*] and NIH 3T3 cells before and at various times after the addition of 1 μM dexamethasone. The duration of dexamethasone treatment (hours) is indicated above the lanes. Northern blots were prepared with 5 μg of total RNA per lane. (A) Upper panel: RNA was isolated from NIH[LTR-*mos*] cells, and the filter was hybridized with a v-*mos*-specific probe. Lower panel: The same filter was rehybridized with a human β-actin probe. (B) Upper panel: αB crystallin-specific 32-mer oligonucleotide (primer 1, see Fig. 5D) was used as the hybridization probe. Lower panel: Section of the acridine orange-stained gel is shown to demonstrate integrity of the RNA and equal loading.

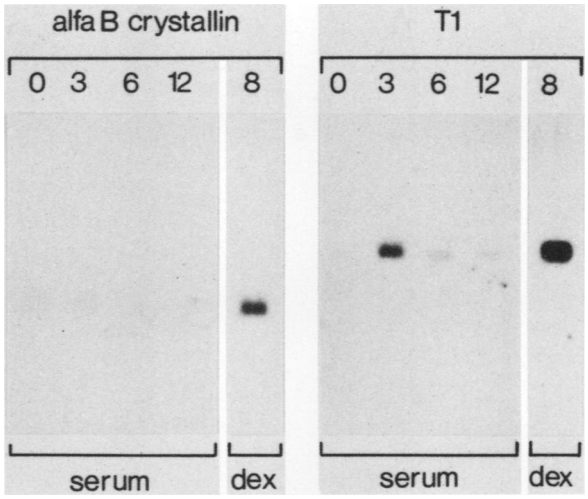

FIG. 4. Serum growth factors do not lead to the accumulation of αB crystallin mRNA. NIH[LTR-*mos*] cells were incubated in the presence of 0.5% FCS for 24 h. Thereafter, the serum concentration was raised to 10% and RNA was isolated after the times (hours) indicated above the lanes. In parallel, logarithmically growing cells were stimulated with dexamethasone (dex) for 8 h. The same filter was hybridized in succession with an αB crystallin (left side)- and a T1 (right side)-specific probe.

expressing cells. To test whether v-*mos* oncoprotein-mediated αB crystallin transcription is initiated at the same site in NIH 3T3 cells as it is in the lens epithelium, we performed primer extension experiments using as a primer the same oligonucleotide as for Northern blot hybridization. This primer was extended by approximately 15 nucleotides on the RNA from dexamethasone-treated NIH[LTR-*mos*] cells. If RNA from untreated cells was used as the template instead, only a very low amount of the extension product was produced (Fig. 5A). To precisely locate the 5′ end of the mRNA, we performed primer extension reactions in the presence of dideoxynucleoside triphosphates. The major 5′ end was found to map to the same position as that of αB crystallin mRNA isolated from mouse eye lens epithelial cells (9) (Fig. 5B, left panel). Upon longer exposure of the gel, a second start site approximately 50 nucleotides further upstream was revealed. The sequence past the major start site (Fig. 5B) is identical to the published mouse αB crystallin sequence upstream of the transcription initiation site (9). We synthesized a second oligonucleotide complementary to the 5′ region flanking the major start site (Fig. 5D, primer 2). It was used in primer extension experiments to map this upstream start site more precisely and, in addition, to verify that the major primer extension product indeed originated from the termination of reverse transcriptase at a transcriptional initiation site and not at a secondary structure barrier of the RNA. Such a putative barrier should be overcome by the extension of a primer which hybridizes to sequences upstream of it. This second primer oligonucleotide was extended by 18 nucleotides. This finding maps the upstream start site to position −49 (Fig. 5C and D). The much lower abundance of this extension product clearly demonstrates that transcription initiates predominantly at the proximal site. TATA boxes are found 28 and 26 nucleotides upstream of the major and minor start sites, respectively. From the results of primer extension experiments, Dubin et al. (9) have previously suggested that transcription initiates at two sites on the αB crystallin gene in heart and skeletal muscle cells. Besides these two start sites, there appear to be two additional very weak transcription initiation sites further upstream as revealed from the two faint bands in the last lane of Fig. 5B above position −49.

Sequence of αB crystallin cDNA. We wished to confirm the identity between the αB crystallin mRNAs from eye lens epithelia and from NIH[LTR-*mos*] cells. To prove this identity, we isolated cDNA clones derived from mRNAs which were extracted from NIH[LTR-*mos*] cells and from mouse lenses with the help of the PCR. In addition, we cloned the αB crystallin cDNA from the larger-sized mRNA in brain and heart muscle. We used an oligonucleotide which represents a part of the 5′ untranslated region including the initiation codon and an oligo(dT) adaptor as primers. This

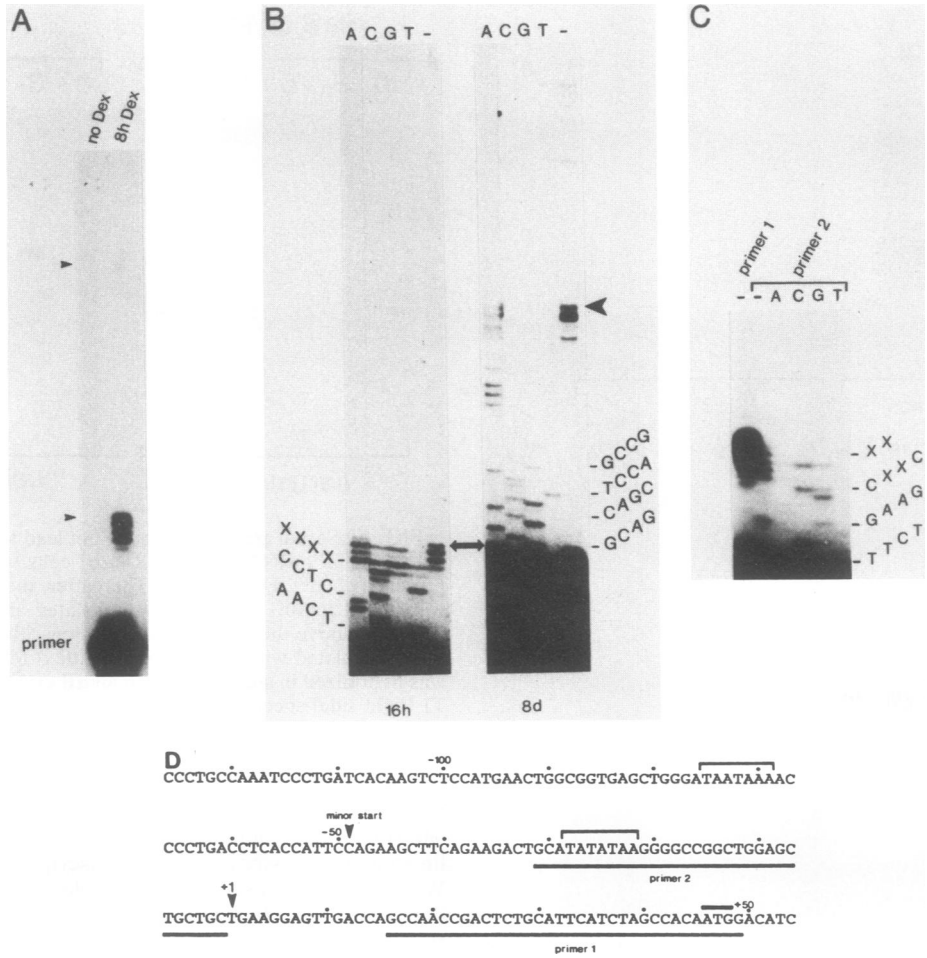

FIG. 5. Mapping of the 5′ ends of αB crystallin mRNA in v-*mos*-expressing cells. (A) Primer extension with primer 1. The primer (complementary to the sequence positions 16 to 49 of αB crystallin, panel D) was extended on total RNA isolated from NIH[LTR-*mos*] cells. These cells were left untreated (no dexamethasone [Dex]) or were stimulated with dexamethasone for 8 h before the extraction of the RNA. (B) Sequence of the extended primer 1. The reverse transcription reactions were performed in the presence or absence of dideoxynucleoside triphosphates. The dideoxynucleoside triphosphates present during the primer extension reactions are indicated at the top of the figure. The deduced sequence (complementary to the mRNA sequence, which is given in panel D) is indicated at the side of the figure. The gel was exposed for 16 h (left panel) and 8 days (right panel). Only part of the sequence past the major start site can clearly be read on the long exposure due to low dideoxynucleoside triphosphate concentrations. The arrow and arrowhead point to the major and minor start sites, respectively. (C) Primer extension with primer 2. The same experiments as described above were performed with primer 2 (complementary to the sequence positions −1 to −31, panel D). A primer extension reaction with primer 1, using the same amount of template RNA as in all the other reactions, was added for comparison. (D) Sequence of the mouse αB crystallin gene around the transcription initiation sites. The regions complementary to the two primer oligonucleotides are underlined. The two TATA boxes and the translation initiation codon are emphasized. The arrowheads point to the major (+1) and minor transcription start sites. The nucleotide sequence is from Dubin et al. (9).

latter primer can hybridize to the poly(A) tail of all mRNAs and was also used for the cDNA synthesis. A single PCR product of approximately 700 bp was obtained from all cDNA preparations. The 3′ parts of clones derived from the various RNA sources were sequenced and found to be identical. Thus, all αB crystallin mRNAs are polyadenylated at the same position. The larger size of the brain and lung mRNAs can therefore be attributed neither to different polyadenylation site selection nor to differential splicing, as we obtained identically sized PCR products. Thus, αB crystallin gene transcription in brain and lung tissue is either initiated further upstream or the different mRNA size is due to variable lengths of the poly(A) tails.

The complete sequence of the cDNA derived from NIH[LTR-*mos*] cells was derived (Fig. 6). The nucleotide sequence was strongly conserved between the hamster, human, mouse, and rat cDNAs, particularly within the coding region. An even stronger conservation was observed at the protein level (Fig. 2). The hamster and mouse sequences differed at only four positions. Variations at three of these positions were also observed in human and/or bovine αB crystallin. The alteration near the carboxy terminus (threonine to alanine) which is unique to the mouse sequence and which lies within the region of the protein which was used to raise the antiserum, which we utilized in later experiments (see below), was verified by sequencing four different clones derived from independent PCRs.

Detection of αB crystallin in v-*mos* oncogene-expressing

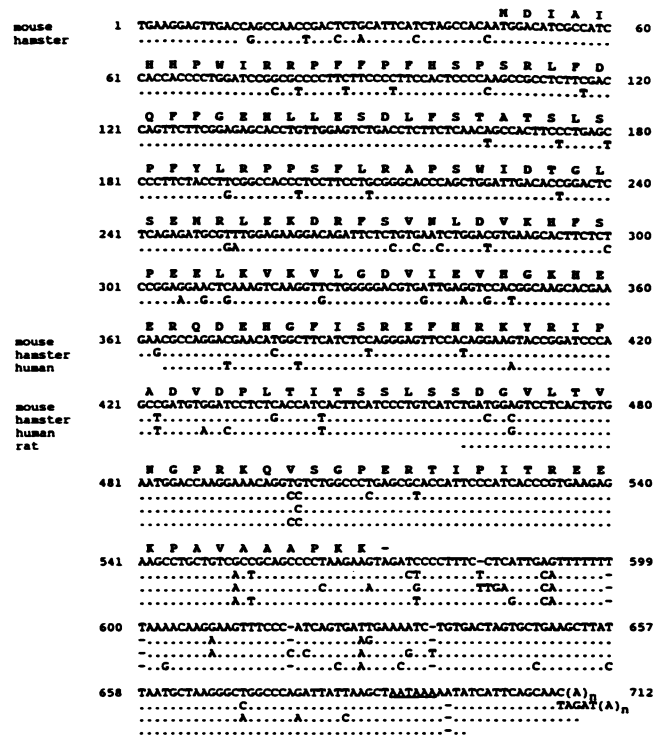

FIG. 6. Sequence of mouse αB crystallin cDNA. The sequence displayed in the upper lane was obtained from a cDNA clone representing mRNA from dexamethasone-stimulated NIH[LTR-*mos*] cells. It is compared with the αB crystallin sequences of hamster (43), human (18), and rat (3). The sequence of the first 48 nucleotides (from the start site to the initiation codon) is taken from Dubin et al. (9). The sense-strand-specific PCR primer spans the region of nucleotides 19 to 48.

cells. To confirm the identity between p23 and αB crystallin at the polypeptide level, we performed Western blot experiments with protein extracts from untreated and dexamethasone-stimulated NIH 3T3 and NIH[LTR-*mos*] cells. The antiserum raised against a decapeptide representing the carboxy terminus of hamster, human, and rat αB crystallin was kindly provided by J. Horwitz. This antiserum does not recognize αA crystallin (31). As expected, the v-*mos* oncogene expression led to the accumulation of a protein which reacts with the antiserum and which migrates on an SDS-polyacrylamide gel to the same position as αB crystallin from mouse eye lenses (Fig. 7A, upper panel). Only small amounts of αB crystallin were detected in NIH 3T3 cells at late times after hormone stimulation (Fig. 7A, lower panel). A second, more slowly migrating immunoreactive protein was consistently observed. Preabsorption of the antiserum with a mouse eye lens protein extract reduced the reaction of the serum with the hormone-inducible lower band only, indicating that the constitutively expressed, more slowly migrating protein does not share an antigenic determinant with αB crystallin (Fig. 7B).

We have previously shown that the synthesis of p23 (αB crystallin) is also induced following the expression of a dexamethasone-inducible Ha-*ras*(EJ) oncogene (21). Here we verified by Western blot analysis that αB crystallin synthesis indeed occurs after the induction of the Ha-*ras* oncogene (Fig. 7C).

DISCUSSION

Identification of p23 as αB crystallin. The data presented in this report lead us to conclude that the 23-kDa protein (p23) which accumulates in v-*mos*- and Ha-*ras*(EJ)-expressing cells is αB crystallin. This conclusion is based on the following evidence. (i) The size of p23 as determined from its migration on SDS-polyacrylamide gels corresponds precisely with the size of αB crystallin. (ii) The amino-terminal sequence of the two p23-derived cyanogen bromide cleavage products are identical with αB crystallin sequences. (iii) Northern blot analysis and primer extension experiments indicated that bona fide αB crystallin mRNA accumulates after the induction of the v-*mos* oncogene in NIH 3T3 cells. (iv) The isolation of cDNA clones which encode authentic αB crystallin was possible by using cDNA copies of the mRNA population from v-*mos*-expressing fibroblasts. (v) αB crystallin could be detected immunologically in NIH 3T3 cells following the activation of the v-*mos* and the Ha-*ras* oncogenes.

α crystallins are major protein components of the eye lens (for recent reviews, see references 41 and 62). The two α crystallins, αA and αB, are closely related, with almost 60% sequence identity (58). They are each encoded by a single gene. The αA crystallin promoter is exclusively active in the cells of the eye lens as revealed by experiments with transgenic animals harboring an αA crystallin-*cat* transgene (27, 38). It was recently demonstrated that this tight restriction of gene expression does not hold true for the αB crystallin gene (3, 9, 18, 26a). Besides the very high concentration in the eye lens, substantial amounts of αB crystallin have been observed in muscular tissues and, to a lesser extent, in lung, kidney, spinal cord, and brain. Furthermore, αB crystallin gene expression has been demonstrated in scrapie-infected hamster brain cells (10). αB crystallin was shown to be the major protein constituent of Rosenthal fibers found in astrocytes of patients suffering from Alexander's disease (18). Several taxon-specific eye lens crystallin genes have a rather broad expression pattern as well. They encode proteins which have recently been identified as housekeeping enzymes involved in intermediary metabolism (for reviews, see references 6, 8, 41, 42, 62). The very high abundance of αB crystallin in the lens suggests a structural rather than an enzymatic function in that tissue. This phenomenon, known as gene sharing, is widespread and observed not only in mammals but also in cephalopods, whose eyes have evolved in quite a different manner (57). The nonlenticular expression of the αB crystallin gene raises the possibility that its product serves a dual function as well.

What is the nonlenticular function of αB crystallin? In contrast to most oncoprotein-responsive genes, αB crystallin gene expression is not triggered by serum growth factors. Therefore, αB crystallin is probably not directly involved in the proliferation response to oncogene expression. It is tempting to speculate that αB crystallin has an enzymatic activity involved in some aspects of metabolic alterations which go along with oncogenic transformation.

The expression of oncogenes is often associated with the synthesis of heat shock proteins (HSPs) (20, 25, 32, 37), indicating that neoplastic transformation shares at least some aspects with other stressful conditions. We have previously demonstrated that αB crystallin synthesis is heat inducible (21). We have further observed that Cd^{2+}, another strong inducer of the heat shock response, leads to the synthesis of αB crystallin as well (unpublished data). In light of these observations, it is interesting to note the striking

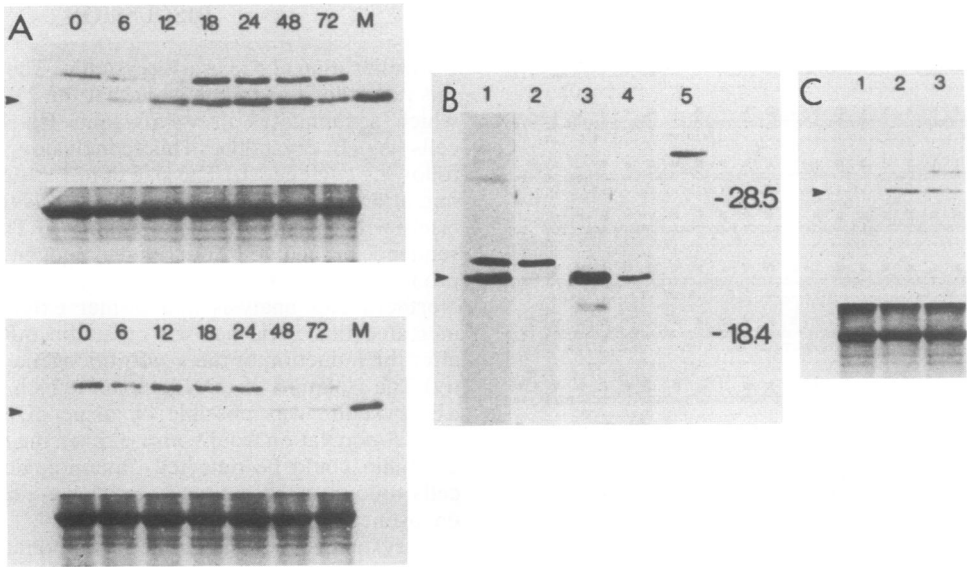

FIG. 7. Immunological detection of αB crystallin. (A) NIH[LTR-*mos*] cells (upper panel) and NIH 3T3 cells (lower panel) either received no dexamethasone or were grown in the presence of 1 μM dexamethasone for the times indicated above the figure (hours). Samples (10 μg) of the protein extracts were subjected to electrophoresis through an SDS-12.5% polyacrylamide gel and to Western immunoblot analysis. The positions of αB crystallin in all parts of this figure are indicated by the arrowheads. A protein extract from mouse eye lens was run in the control lane (lane M). The upper part of the polyacrylamide gel was cut off and stained with Coomassie brilliant blue. A segment of the stained gels is depicted below the Western immunoblots in this panel as well as in panel C of this figure to demonstrate equal loading of protein. (B) Protein extract (50 μg) isolated from NIH[LTR-*mos*] cells which were treated with dexamethasone for 1 day (lanes 1, 2, and 5) and 0.5 μg of mouse eye lens protein extract were subjected to Western immunoblot analysis. Untreated αB crystallin-specific antiserum was used for lanes 1 and 3. This same antiserum was preincubated with a mouse eye lens protein extract (50 μg) for 1 h before incubation with the Western immunoblot (lanes 2 and 4). A nonimmune rabbit serum was reacted with the filter displayed in lane 5. The arrowhead indicates the position of αB crystallin. The positions of molecular weight markers ($\times 10^3$) are given at the side of the figure. (C) NIH[LTR-*ras*(EJ)] cells either received no dexamethasone (lane 1) or received dexamethasone for 1 day (lane 2) or 2 days (lane 3).

sequence similarity between α crystallins and small HSPs (16, 17, 53, 61). The relationship extends beyond the primary amino acid sequence. αB crystallin and the small HSPs form supramolecular structures with the same sedimentation coefficient and identical morphology as detected by electron microscopy (1, 2, 33). Moreover, we have observed the cosedimentation of αB crystallin with nuclei under heat shock conditions (unpublished data). The same phenomenon has been described for small HSPs and has been taken as evidence for the association of these proteins with the intermediate filament, which collapses onto the nucleus under these conditions (1). It is interesting that heart muscle αB crystallin colocalizes with the intermediate filament as well (26a). All these similarities between αB crystallin and the small HSPs suggest a functional relationship. Unfortunately, despite intense research, the function of the small HSPs remains a mystery. Their genes are induced during normal development as well as under stress conditions (for a recent review, see reference 26). Their involvement in the establishment of cellular stress tolerance has variously been suggested, but the issue is still a matter of debate (40, 56).

The accumulation of αB crystallin in our experimental system is transient. The down-regulation which follows the oncoprotein-mediated induction can probably not be attributed to the repression of the MMTV LTR-driven oncogenes shortly after their induction with dexamethasone, since we could not detect substantial amounts of αB crystallin in transformed NIH 3T3 cell lines constitutively expressing the Ha-*ras* or v-*mos* oncogene (data not shown). The transient expression of αB crystallin is reminiscent of the expression pattern of many growth factor-inducible immediate-early genes, whose activity is restricted to a short period during the transition from the G0 to the G1 phase of the cell cycle. The proteins which they encode presumably fulfill a function which is needed mainly during this transition period. Likewise, αB crystallin might only be required during a short period following the activation of oncogenes, when drastic changes of the cellular morphology and biochemistry are included.

ACKNOWLEDGMENTS

We thank J. Horwitz for the αB crystallin antiserum and R. Jaggi for the NIH[LTR-*mos*] and NIH[LTR-*ras*(EJ)] cell lines. We thank C. Remé for help with the eye lens dissection and C. Wickenden for critical reading of this manuscript.

This project was supported by the Swiss National Science Foundation (grant 31-25294.88 to R.K.) and initially by the Ludwig Institute for Cancer Research, Berne Branch. A.A. is the recipient of a fellowship from the Cancer League of the Kanton of Zurich.

REFERENCES

1. **Arrigo, A.-P., J. P. Suhan, and W. J. Welch.** 1988. Dynamic changes in the structure and intracellular locale of the mammalian low-molecular-weight heat shock protein. Mol. Cell. Biol. **8**:5059–5071.
2. **Arrigo, A.-P., and W. J. Welch.** 1987. Characterization and purification of the small 28000-dalton mammalian heat shock protein. J. Biol. Chem. **262**:15359–15369.
3. **Bhat, S. P., and C. N. Nagineni.** 1989. Alfa B subunit of lens-specific protein alfa-crystallin is present in other ocular and non-ocular tissues. Biochem. Biophys. Res. Commun. **158**:319–325.

4. **Bonner, W., and R. A. Laskey.** 1974. A film detection method of tritium-labeled proteins and nucleic acids in polyacrylamide gels. Eur. J. Biochem. **46**:83–88.
5. **Chomczynski, P., and N. Sacchi.** 1987. Single-step method of RNA isolation by acid guanidinium thiocyanate-phenol-chloroform extraction. Anal. Biochem. **162**:156–159.
6. **deJong, W. W., W. Hendriks, J. W. M. Mulders, and H. Bloemendal.** 1989. Evolution of eye lens crystallins: the stress connection. Trends Biochem. Sci. **14**:365–368.
7. **DeLarco, J. E., and G. J. Todaro.** 1978. Growth factors from murine sarcoma virus-transformed cells. Proc. Natl. Acad. Sci. USA **75**:4001–4005.
8. **Doolittle, R. F.** 1988. More molecular opportunism. Nature (London) **336**:18–19.
9. **Dubin, R. A., E. F. Wawrousek, and J. Piatigorsky.** 1989. Expression of the murine alfa B-crystallin gene is not restricted to the lens. Mol. Cell. Biol. **9**:1083–1091.
10. **Duguid, J. R., R. G. Rohwer, and B. Seed.** 1988. Isolation of cDNAs of scrapie-modulated RNAs by subtractive hybridization of a cDNA library. Proc. Natl. Acad. Sci. USA **85**:5738–5742.
11. **Feinberg, A. P., and B. Vogelstein.** 1983. A technique for radiolabeling DNA restriction endonuclease fragments to high specific activity. Anal. Biochem. **132**:6–13.
12. **Feinberg, A. P., and B. Vogelstein.** 1984. Addendum to: A technique for radiolabeling DNA restriction endonuclease fragments to high specific activity. Anal. Biochem. **137**:266–267.
13. **Feramisco, J. R., M. Gross, T. Kamata, M. Rosenberg, and R. W. Sweet.** 1984. Microinjection of the oncogene form of the human H-*ras* (T-24) protein results in rapid proliferation of quiescent cells. Cell **38**:109–117.
14. **Gottesman, M. M.** 1978. Transformation-dependent secretion of a low molecular weight protein by murine fibroblasts. Proc. Natl. Acad. Sci. USA **75**:2767–2771.
15. **Herschman, H. R.** 1989. Extracellular signals, transcriptional responses and cellular specificity. Trends Biochem. Sci. **14**:455–458.
16. **Hickey, E., S. E. Brandon, R. Potter, G. Stein, J. Stein, and L. A. Weber.** 1986. Sequence and organization of genes encoding the human 27 kDa heat shock protein. Nucleic Acids Res. **14**:4127–4145.
17. **Ingolia, T. D., and E. A. Craig.** 1982. Four small Drosophila heat shock proteins are related to each other and to mammalian alfa-crystallin. Proc. Natl. Acad. Sci. USA **79**:2360–2364.
18. **Iwaki, T., A. Kume-Iwaki, R. K. H. Liem, and J. E. Goldman.** 1989. Alfa B-crystallin is expressed in non-lenticular tissues and accumulates in Alexander's disease brain. Cell **57**:71–78.
19. **Jaggi, R., B. Salmons, D. Muellenêr, and B. Groner.** 1986. The v-mos and H-ras oncogene expression represses glucocorticoid hormone-dependent transcription from the mouse mammary tumor virus LTR. EMBO J. **5**:2609–2616.
20. **Kingston, R. E., A. S. Baldwin, Jr., and P. A. Sharp.** 1984. Regulation of heat shock protein 70 gene expression by c-myc. Nature (London) **312**:280–282.
21. **Klemenz, R., S. Hoffmann, R. Jaggi, and A.-K. Werenskiold.** 1989. The v-mos and c-Ha-ras oncoproteins exert similar effects on the pattern of protein synthesis. Oncogene **4**:799–803.
22. **Klemenz, R., S. Hoffmann, and A.-K. Werenskiold.** 1989. Serum- and oncoprotein-mediated induction of a gene with sequence similarity to the gene encoding carcinoembryonic antigen. Proc. Natl. Acad. Sci. USA **86**:5708–5712.
23. **Kramps, J. A., B. M. deMan, and W. W. deJong.** 1977. The primary structure of the B2 chain of human alfa-crystallin. FEBS Lett. **74**:82–84.
24. **Laemmli, U. K.** 1970. Cleavage of structural proteins during the assembly of the head of bacteriophage T4. Nature (London) **227**:680–685.
25. **LaThanque, N. B., and D. S. Latchman.** 1988. A cellular protein related to heat-shock protein 90 accumulates during herpes simplex virus infection and is overexpressed in transformed cells. Exp. Cell Res. **178**:169–179.
26. **Lindquist, S., and E. A. Craig.** 1988. The heat-shock proteins. Annu. Rev. Genet. **22**:631–677.
26a. **Longoni, S., S. Lattonen, G. Bullock, and M. Chiesi.** 1990. Cardiac alpha-crystallin. Intracellular localization. Mol. Cell. Biochem. **97**:121–128.
27. **Mahon, J. A., A. B. Chepelinsky, J. S. Khillan, P. A. Overbeek, J. Piatigorsky, and H. Westphal.** 1987. Oncogenesis of the lens in transgenic mice. Science **235**:1622–1628.
28. **Matrisian, L. M., N. Glaichenhaus, M.-C. Gesnel, and R. Breathnach.** 1985. Epidermal growth factor and oncogenes induce transcription of the same cellular mRNA in rat fibroblasts. EMBO J. **4**:1435–1440.
29. **McMaster, G. K., and G. G. Carmichael.** 1977. Analysis of single- and double-stranded nucleic acids on polyacrylamide and agarose gels by using glyoxal and acridine orange. Proc. Natl. Acad. Sci. USA **74**:4835–4838.
30. **Morrissey, J. H.** 1981. Silver stain for proteins in polyacrylamide gels. A modified procedure with enhanced uniform sensitivity. Anal. Biochem. **117**:307–310.
31. **Nagineni, C. N., and S. P. Bhat.** 1988. Maintenance of the synthesis of alfa B-crystallin and progressive expression of beta Bp-crystallin in human fetal lens epithelial cells in culture. Dev. Biol. **130**:402–405.
32. **Nevins, J. R.** 1982. Induction of the synthesis of a 70,000 dalton mammalian heat shock protein by the adenovirus E1A gene product. Cell **29**:913–919.
33. **Nover, L., K. D. Scharf, and D. Neumann.** 1989. Cytoplasmic heat shock granules are formed from precursor particles and contain a specific set of mRNAs. Mol. Cell. Biol. **9**:1298–1308.
34. **Nunez, A.-M., M. Berry, J. L. Imler, and P. Chambon.** 1989. The 5′ flanking region of the pS2 gene contains a complex enhancer region responsive to oestrogens, epidermal growth factor, a tumor promoter (TPA), the c-Ha-ras oncoprotein and the c-jun protein. EMBO J. **8**:823–829.
35. **O'Farrell, P. H.** 1975. High resolution two-dimensional electrophoresis of proteins. J. Biol. Chem. **250**:4007–4021.
36. **O'Farrell, P. Z., H. M. Goodman, and P. H. O'Farrell.** 1977. High resolution two-dimensional electrophoresis of basic as well as acidic proteins. Cell **12**:1133–1142.
37. **Omar, R. A., and K. W. Lanks.** 1984. Heat shock protein synthesis and cell survival in clones of normal and simian virus 40-transformed mouse embryo cells. Cancer Res. **44**:3976–3982.
38. **Overbeek, P. A., A. B. Chepelinsky, J. S. Khillan, J. Piatigorsky, and H. Westphal.** 1985. Lens-specific expression and developmental regulation of the bacterial chloramphenicol acetyltransferase gene driven by the murine alfa A-crystallin promoter in transgenic mice. Proc. Natl. Acad. Sci. USA **82**:7815–7819.
39. **Owen, R. D., and M. C. Ostrowski.** 1987. Rapid and selective alterations in the expression of cellular genes accompany conditional transcription of Ha-v-*ras* in NIH 3T3 cells. Mol. Cell. Biol. **7**:2512–2520.
40. **Petko, L., and S. Lindquist.** 1986. Hsp26 is not required for growth at high temperatures, nor for thermotolerance, spore development, or germination. Cell **45**:885–894.
41. **Piatigorsky, J.** 1989. Lens crystallins and their genes: diversity and tissue-specific expression. FASEB J. **3**:1933–1940.
42. **Piatigorsky, J., and G. J. Wistow.** 1989. Enzyme/crystallins: gene sharing as an evolutionary strategy. Cell **57**:197–199.
43. **Quax-Jeuken, Y., W. Quax, G. van Rens, P. M. Khan, and H. Bloemendal.** 1985. Complete structure of the alfa B-crystallin gene: conservation of the exon-intron distribution in the two nonlinked alfa-crystallin genes. Proc. Natl. Acad. Sci. USA **82**:5819–5823.
44. **Rollins, B. J., and C. D. Stiles.** 1989. Serum-inducible genes. Adv. Cancer Res. **53**:2–32.
45. **Sanger, F., and A. R. Coulson.** 1978. The use of thin acrylamide gels for DNA sequencing. FEBS Lett. **87**:107–110.
46. **Sanger, F., S. Nicklen, and A. R. Coulson.** 1977. DNA sequencing with chain-terminating inhibitors. Proc. Natl. Acad. Sci. USA **74**:5463–5467.
47. **Schaffner, W., and C. Weissmann.** 1973. A rapid, sensitive, and specific method for the determination of protein in dilute solution. Anal. Biochem. **56**:502–514.
48. **Schönthal, A., P. Herrlich, H. J. Rahmsdorf, and H. Ponta.** 1988. Requirement for fos gene expression in the transcriptional

activation of collagenase by other oncogenes and phorbol esters. Cell **54**:325–334.
49. **Simpson, R. J., R. L. Moritz, E. C. Nice, and B. Grego.** 1987. A high-performance liquid chromatography procedure for recovering subnanomole amounts of protein from SDS-gel electroeluantes for gas-phase sequence analysis. Eur. J. Biochem. **165**:21–29.
50. **Simpson, R. J., R. L. Moritz, M. R. Rubira, and J. Van Snick.** 1989. Complete amino acid analysis of a new murine T-cell growth factor P40. Eur. J. Biochem. **183**:715–722.
51. **Simpson, R. J., and E. C. Nice.** 1984. In situ cyanogen bromide cleavage of N-terminally blocked proteins in a gas-phase sequenator. Biochem. Int. **8**:787–791.
52. **Sistonen, L., E. Hölttä, T. P. Mäkelä, J. Keski-Oja, and K. Alitalo.** 1989. The cellular response to induction of the p21 c-Ha-ras oncoprotein includes stimulation of jun gene expression. EMBO J. **8**:815–822.
53. **Southgate, R., A. Ayme, and R. Voellmy.** 1983. Nucleotide sequence analysis of the Drosophila small heat shock gene cluster at locus 67B. J. Mol. Biol. **165**:35–57.
54. **Stacey, D. W., T. Watson, H.-F. Kung, and T. Curran.** 1987. Microinjection of transforming *ras* protein induces c-*fos* expression. Mol. Cell. Biol. **7**:523–527.
55. **Sugano, S., M. Y. Stoeckle, and H. Hanafusa.** 1987. Transformation by Rous sarcoma virus induces a novel gene with homology to a mitogenic platelet protein. Cell **49**:321–328.
56. **Susek, R. E., and S. L. Lindquist.** 1989. Hsp26 of *Saccharomyces cerevisiae* is related to the superfamily of small heat shock proteins but is without a demonstratable function. Mol. Cell. Biol. **9**:5265–5271.
57. **Tomarev, S. I., and R. D. Zinovieva.** 1988. Squid major lens polypeptides are homologous to glutathione *S*-transferase subunits. Nature (London) **336**:86–88.
58. **van der Ouderaa, F. J., W. W. de Jong, A. Hilderink, and H. Bloemendal.** 1974. The amino-acid sequence of the alfa B2 chain of bovine alfa crystallin. Eur. J. Biochem. **49**:157–168.
59. **Wasylyk, C., J. L. Imler, J. Perez-Mutul, and B. Wasylyk.** 1987. The c-Ha-ras oncogene and a tumor promoter activate the polyoma virus enhancer. Cell **48**:525–534.
60. **Werenskiold, A.-K., S. Hoffmann, and R. Klemenz.** 1989. Induction of a mitogen-responsive gene after expression of the Ha-*ras* oncogene in NIH 3T3 fibroblasts. Mol. Cell. Biol. **9**:5207–5214.
61. **Wistow, G.** 1985. Domain structure and evolution in alfa crystallins and small heat-shock proteins. FEBS Lett. **181**:1–6.
62. **Wistow, G. J., and J. Piatigorsky.** 1988. Lens crystallins: the evolution and expression of proteins for a highly specialized tissue. Annu. Rev. Biochem. **57**:479–504.